HHS Public Access

Author manuscript

J Immunol. Author manuscript; available in PMC 2020 October 15.

Published in final edited form as:

J Immunol. 2019 October 15; 203(8): 2063–2075. doi:10.4049/jimmunol.1900399.

Early KLRG1^{+} but not CD57^{+}CD8^{+} T cells in Primary CMV Infection Predict Effector Function and Viral Control

Aki Hoji[#,*], **Iulia D. Popescu**[#,*], **Mathew R. Pipeling**[#], **Pali D. Shah**[&], **Spencer A. Winters**[#], **John F. McDyer**[#]

[#]Division of Pulmonary, Allergy, and Critical Care Medicine, Department of Medicine, University of Pittsburgh School of Medicine, Pittsburgh, Pennsylvania, 15213, USA [&]Division of Pulmonary and Critical Care Medicine, Department of Medicine, Johns Hopkins University School of Medicine, Baltimore, Maryland [*]Both authors contributed equally to this work

Abstract

CMV remains an important opportunistic pathogen in high-risk lung transplant recipients (LTRs). We characterized the phenotype and function of CD8^{+} T cells from acute/primary into chronic CMV infection in 23 (donor+/recipient-; D+R-) LTRs and found rapid induction of both KLRG1^{+} and/or CD57^{+} CMV-specific CD8^{+} T cells with unexpected co-expression of CD27. These cells demonstrated maturation from an acute effector (T_{AEFF}) to an effector memory (T_{EM}) phenotype with progressive enrichment of KLRG1^{+}CD57^{+}CD27^{-} cells into memory. CMV-specific KLRG1^{+} T_{AEFF} cells were capable of *in vitro* proliferation that diminished upon acquisition of CD57, whereas only KLRG1^{+} expression correlated with T-bet expression and effector function. In contrast to blood T_{AEFF} cells, lung mucosal T_{AEFF} cells demonstrated reduced KLRG1/T-bet expression but similar CD57 levels. Additionally, increased KLRG1$^{+}T_{AEFF}$ cells were associated with early immune viral control following primary infection. Together, our findings provide new insights into the roles of KLRG1 and CD57 expression in human T cells, forming the basis for a refined model of CD8^{+} T cell differentiation during CMV infection.

INTRODUCTION

Cytomegalovirus (CMV), a member of the β-herpesvirus family, remains a significant opportunistic pathogen and cause of morbidity and mortality in solid organ and hematopoietic cell transplant recipients. Lung transplant recipients (LTRs), in particular seronegative recipients of allografts from seropositive donors (donor+/recipient-;D+R-), are

Correspondence: John F. McDyer, M.D., Associate Professor of Medicine, Division of Pulmonary, Allergy, and Critical Care Medicine, University of Pittsburgh School of Medicine, 3459 Fifth Avenue, NW 628, Pittsburgh, PA, 15213, Phone: (412) 624-8915, Fax: (412) 692-2260, mcdyerjf@upmc.edu.

Author's contributions

A. Hoji, I.D. Popescu, and J.F. McDyer designed and analyzed experiments. A. Hoji, and I.D. Popescu performed, analyzed and interpreted results. A. Hoji wrote a majority of the manuscript, and I.D. Popescu contributed figure legends, methods. M.R. Pipeling and P.D. Shah provided clinical specimen and patients' characteristics. I.D. Popescu and S.A. Winters compiled patient data. J.F. McDyer supervised the study, and edited the manuscript.

Competing financial interests

Authors declare no competing financial interests.

at increased risk for CMV complications (1) (2). CMV infectious complications such as pneumonitis and viremia have been implicated in LTRs as risk factors for developing chronic lung allograft dysfunction (CLAD) and the bronchiolitis obliterans syndrome (BOS), the major limiting factor for long-term survival in LTRs (3–5). Despite the adoption of extended antiviral prophylaxis strategies in the past decade in many transplant programs, D+R-LTRs (6), who comprise 25% of all LTRs, continue to demonstrate increased risk for recurrent CMV viremia, CMV end-organ disease and increased 5-year mortality (7). We have previously demonstrated heterogeneity of CMV-specific T cell immunity among the D+R-LTR population that is predictive of the capacity for early viral control following primary infection. Specifically, we have shown important roles for induction of the major Type-1 transcription factor T-bet, effector function and proliferative capacity in $CD8^+$ and $CD4^+$ T cells as significant functional immune correlates for establishing viral control during early chronic CMV infection (8) (9) (10). Recently, we showed that idiopathic pulmonary fibrosis lung recipients with short telomeres demonstrate impaired CMV-specific T cell immunity and T-bet induction that correlated with increased risk for CMV complications (11). However, questions remain as to the optimal T cell marker(s) that could prospectively stratify high-risk lung recipients who are at risk for relapsing CMV following discontinuation of antiviral therapy versus those with the capacity to establish immune control. Lung transplantation provides a unique opportunity to evaluate viral immune mechanisms as the advent of primary CMV infection is often known and both peripheral and allograft-derived resident T cells can be tracked into chronic infection (12, 13).

Similar to virus-specific $CD8^+$ T cells in the mouse, a linear progression in differentiation is the current paradigm in human T cells (14) (15) (16). However, while the phenotype and function of effector memory (T_{EM}) CMV-specific $CD8^+$ T cells during chronic infection has been widely investigated, the phenotypic correlates of $CD8^+$ T_{EFF} function during acute/primary CMV infection have been less characterized. Early studies showed that CMV-specific $CD8^+$ T cells during chronic infection are enriched predominantly in the mature effector memory phenotype $CD27^-CD28^-CD45RA^{hi}$, marked by the increased expression of granzymes A/B, perforin and IFN-γ, but a diminished proliferative capacity (17–19). In parallel, these cells acquire surface expression of the terminal differentiation markers, co-inhibitory receptor killer cell lectin-like receptor subfamily G member 1 (KLRG1) (20), and CD57 (21, 22). Acquisition of CD57 expression is thought to occur increasingly over the course of chronic CMV infection (16) (23) while persistence of CMV antigen is thought to drive progressive downregulation of CD27 into the effector memory phase (24).

In the acute/primary LCMV mouse infection model, $KLRG1^{hi}$ surface expression marks short-lived effector cells (SLECs) that are critical for rapid viral clearance and its expression is T-bet dependent (25). While both KLRG1 and CD57 (no mouse equivalent) are expressed in human memory $CD8^+$ T cells (26), and most notably in CMV-specific $CD8^+$ T cells (27) (28), expression and potential functional correlation of these markers of terminal differentiation have not been evaluated during acute/primary viral infection. Based on our previous findings showing early T-bet induction in $CD8^+$ T cells during acute/primary CMV infection and its importance in viral control (8) (9), we hypothesized that an early induction of KLRG1 and/or CD57 in CMV-specific $CD8^+$ T cells correlates with effector function and the early establishment of CMV control.

In this study, we characterized the phenotypic and functional capacity of CMV-specific $CD8^+$ T cells during acute/primary CMV infection into chronic CMV infection in a cohort of D+R-LTRs. We observed rapid induction of both CD57 and KLRG1 surface expression in CMV-specific acute effector $CD8^+$ T cells (T_{AEFF}) during primary CMV infection and *de novo* viremia, surprisingly in conjunction with CD27 co-expression. Importantly, both $CD57^+$ and $KLRG1^+$ CMV-specific $CD8^+$ T_{AEFF} cells demonstrated the capacity for *in vitro* proliferation in response to CMV antigen, however only KLRG1 expression significantly correlated with T-bet and effector multifunction. Further, only the KLRG1 promoter was highly predicted and bound T-bet in a chromatin immunoprecipitation (ChiP) assay and correlated with intracellular T-bet protein expression. Finally, acute KLRG1 induction, but not CD57, expression in CMV-specific $CD8^+$ acute T_{EFF} cells and total acute $CD8^+$ T cells were predictive of the capacity for viral control in D+/R− LTRs during early chronic infection.

MATERIALS AND METHODS

Study participants

D+/R− LTRs from the Johns Hopkins Lung Transplant Program were identified (Table 1) and provided informed written consent for participation in a Johns Hopkins Medicine Institutional Review Board-approved protocol. All patients were treated with standard three-drug immunosuppression. Antiviral prophylaxis with ganciclovir and/or valganciclovir was used for the initial three months after transplant. Patients were prospectively monitored at least weekly for the development of primary CMV infection (defined as *de novo* detection of viral replication by quantitative PCR). CMV viral loads were determined using quantitative PCR of plasma by the Johns Hopkins Hospital Clinical Virology Laboratory. Patients developing primary CMV infection were treated with antiviral therapy (ganciclovir and/or valganciclovir) until two consecutive weekly quantitative CMV PCR measurements revealed undetectable viremia. Following completion of antiviral therapy for primary infection, patients continued to be prospectively monitored with quantitative CMV PCR measured at least biweekly, as well as during any symptomatic or clinically indicated time points, for the development of relapsing viremia (defined as the detection of >300 copies/mL of CMV by quantitative PCR on two consecutive samples after the completion of antiviral therapy for primary infection). Patients with relapsing viremia received antiviral therapy (ganciclovir and/or valganciclovir) if clinically indicated. Dates of chronic and acute viremic samples at minimum of 6 months apart (median ±SEM, 379±69 days; range 184–1096 days). The study was approved by the Institutional Review Board at the University of Pittsburgh.

Preparation of peripheral blood and lung mucosal mononuclear cells (PBMCs and LMNCs)

Blood and BAL samples from LTRs were obtained prior to the discontinuation of initial antiviral prophylaxis (time point referred to as ‘Pre-CMV’) and within 5–14 days of detection of *de novo* viremia (time point referred to as ‘primary CMV’). PBMCs were isolated from heparinized blood samples by density gradient centrifugation using Ficoll-Paque (GE Healthcare) to be used in subsequent assays. Study participants underwent bronchoalveolar lavage (BAL) by use of a standard protocol with instillation of 180 mL of sterile normal saline in the right middle lobe of the lung. A BAL specimen was obtained on

the same day for blood collection. LMMCs were obtained simply via centrifugation of BAL fluid. All patients had therapeutic levels of calcineurin inhibitors at the time of sampling. Cells were then washed with PBS, aliquoted at 10 million cells in 1ml of freezing medium (Invitrogen) and frozen in the liquid nitrogen tank. PBMCs were thawed rapidly in the presence of 2 units per ml of Benzonase (EMD Millipore)

MHC class I dextramer and surface staining of PBMCs and LMNCs

Cryopreserved PBMCs and LMNCs were thawed in in the presence of 2 U/ml of Benzonase (EMD Millipore) and approximately 2×10^6 cells were labeled with FV-510 (BD Biosciences) in IMDM medium (GIBCO) for 10 min at 37°C. Immediately after incubation, cells were washed with the complete medium and stained with the MHC class I dextramer (Immudex, Copenhagen, Denmark) against known immunodominant CMV epitopes (Supp.Table I) at 25°C for 25 min. Cells were then washed and incubated with cocktail of conjugated monoclonal antibodies for 30 min at 4°C in phosphate-buffered saline (PBS) with a fish gelatin blocking reagent (Biotium, Fremont, CA) and 0.1% sodium azide. After the final wash, cells were fixed with 1% paraformaldehyde (Protein Sciences, Meriden, CT) for analysis. Available pre-transplant PBMC samples (Pre-PBMC) were stained with matching MHC class I dextramers (Fig. 1B and Supp Fig.1B) and frequencies of $CD3^+CD8^+$ dextramer positive cells were below 0.01%. Following fluorescent conjugated antibodies were used for staining surface phenotypic markers; CD3-alex700 (UCHT1), CD8-APCH7 (SK1), CD14-BV605 (MSE2), CD16-BV605 (3G8), CD19-BV605 (SJ25C1), CD27-PECy7 (MT271), CD28-PerCPCy5.5 (L293), CD38-BV711 (HIT2), CD45RA-PECy5 (H100), CD57-BV421 (NK-1), CD279 PE-CF594 (EH12.1), CD69-BV650 (FN50), and CD103-BV605 (BerACT8) were purchased from BD Biosciences. T-bet-BV711 (4B10) was purchased from Biolegend. KLRG1-APC (13F12F2) was kindly provided by Dr. Hanspeter Pircher (University of Freiburg, Institute of Immunology).

Flow cytometry

Stained PBMCs or BAL-derived LMNCs were analyzed by the BD Fortessa SORP high-throughput system (HTS). Prior to the acquisition, CountBright Beads (Invitrogen) were added to each well and a fixed volume of the stained sample was acquired by HTS. For visualization of *ex vivo* stained total and CMV-specific $CD8^+$ T cells (Fig. S1A), we used a compounded gating scheme previously described in (23) with a following sequential gate order: potential doublet exclusion based on a FSC-A and FSC-H plot, dead cell exclusion based on the live cell gate on FV-510 and FSC-A plot, inclusion of $CD3^+$ cells based on a $CD3^+$ gate with a $CD14^+CD16^+CD19^+$ exclusion gate on a CD3-Alexa-700 and CD14CD16CD19-QDot605 plot, and a lymphocyte gate on an FSC and SSA log plot. CMV-Specific $CD8^+$ T cells were gated further on MHC class I dextramer positive population on the MHC class I dextramer-PE and SSC-A plot (Supp. Fig. 1A). Data analysis and graphic representations were done with FlowJo v.10 (TreeStar, Ashland, OR).

In vitro short-term stimulation and intracellular cytokine staining (ICS)

Single-pools of overlapping 15-mer peptides for pp65 (JPT, Berlin, Germany) were used. PBMC were cultured in round-bottom tissue culture tubes (Sarstedt) in the presence or absence (medium alone) of pooled pp65 peptides (1μg/mL). All stimulations for intracellular

cytokine production were performed using 10^6 cells per condition for 6 h at 37°C with brefeldin-A (10μg/mL) (Sigma) was added for the final 4 h of culture. Monensin (5 μg/ml) along with brefeldin-A and anti-CD107a-Pacific Blue (Pac Blue) was added at the beginning of culture when CD107a was measured. All cells were collected for flow cytometric analysis with a range of $0.5–1\times10^6$ total events collected per condition. All gates for cytokine frequencies were set using the medium alone control and subtracted from peptide re-stimulated samples frequencies.

In vitro antigen-specific T cell proliferation

Thawed frozen PBMCs were labeled with CytoTell Green (AAT Bioquest) or 0.2 μM CFSE (Invitrogen, Carlsbad, CA) in IMDM medium (GIBCO, Grand Island, NY) for 10 min at 37°C. The cells were immediately washed and plated with IMDM supplemented with 10% FCS in a 96-well plate for 6 days. For antigen-specific stimulation, PBMCs were stimulated in the presence of 2μM single CMV dextramer cognate peptides or the pool of peptide mix for 6 days and then were harvested and prepared for flow cytometric analysis. Proliferating cells were re-stimulated *in vitro* for additional 6 hours with the CMV-specific pp65 peptide pool and assessed for proliferation via simultaneous CFSE dilution and cytokine production by ICS. Based on the Boolean gating analysis, cytokine co-expression was determined by using SPICE (29).

Chromatin immune-precipitation (ChIP) assay

The Chip assay was performed by using Zymo-Spin™ ChIP kit according to manufacturer's recommendation with modifications based on published protocols (30)(31). Briefly, 5–6 $\times10^6$ cells were fixed in 1% paraformaldehyde for 10min at 37°C. 2.5M glycine was added to stop the fixation, and then nuclei were extracted. Chromatin in isolated nuclei were digested by Atlantis MNase (Zymo Research) and after digestion, isolated nuclei were mildly sonicated to release digested chromatin. Digested chromatin was then incubated with the ChIP grade mouse monoclonal antibody against human TBX21 (4B10 and D39) (Santa Cruz Biotech), or the control mouse IgG antibody (Santa Cruz Biotech) for overnight at 4°C, and after the incubation, the bound chromatin was immune-precipitated by MagnaChIP protein A+G magnetic beads (EMD Millipore). After series of washes, bound DNA was isolated and stored at −80°C until PCR was performed with sets of primers (Table Supplemental II) to identity the promoter region of the target gene. All the forward and reverse ChIP primer pairs except IL-4 pairs were designed by NCBI Primer-BLAST (32). Sequences of a IL-4 ChIP primer pair were derived from Zhou et.al. (33).

Transcription factor binding site prediction

For prediction of TBX21 DNA binding sites on the KLRG1 promoters, we used a bioconductor R package, TFBSTools (34) with the JASPAR2018 Transcription Factor DNA binding motif database (35) and scan through the promoter region of KLRG1 genomic sequence (ENSG00000139187), 1272 bp upstream of the transcription initiation site (hg38;chr12+:8988175–8989637) and that of B3GAT1 (CD57) genomic sequence (ENSG00000109956), 1429 bp upstream of the transcription start (hg38;chr11-:134413347–134411717). We used the default parameter of a searchSeq tool for scanning potential TBX21 DNA binding sites with a minimum score parameter set at 80%.

Statistical analysis and data visualization

Statistical analysis was performed by using the GraphPad Prism 7 (GraphPad, La Jolla, CA), JMP12 (SAS, Cary, NC) and R (R Core Team, 2018), cytokine co-expression was based on the Boolean gating analysis determined by using SPICE (29). Non-parametric statistical analyses, as indicated, were used and a two-tailed p value of less than 0.05 was considered statistically significant.

Online supplementary materials

A list of single CMV peptide antigens used for in vitro proliferation experiments and MHC class I dextramer staining is found in Supp.Table I. A list of primer sets used in ChIP assay was shown in Supp.Table II. Supp. Fig. 1 shows a compound gating strategy leading to the live CMV pp65-specific MHC class I dextramer^{+}CD3^{+}CD8^{+} cells, and their phenotypic marker expressions from acute primary and chronic samples. Supp. Fig. 2 shows predicted T-bet binding sites using KLRG1 promoter (Supp. Fig.2A) and using B3GAT1 (CD57) promoter (Supp. Fig.2B).

RESULTS

Patient characteristics and clinical phenotypes during and following primary CMV infection in D+R-LTRs

In this study we evaluated the acute CMV-specific CD8^{+} T_{AEFF} cell phenotype and functional responses in a cohort of 23 D+R-LTRs during acute primary CMV infection and a subset into chronic infection. The clinical characteristics of these patients during acute/primary *de novo* viremia are shown in Table 1. Using close prospective monitoring (see Materials and Methods) we detected primary CMV infection at a median of 165 days post-transplant following discontinuation of CMV prophylaxis therapy. Prospective, standard of care monitoring in this high-risk population continued and detected relapsing viremia in 10 LTRs (relapsers; 43.4%) within the first 6 months of early chronic infection in contrast to 13 LTRs who demonstrated immune control (controllers; 56.5%) following discontinuation of antiviral therapy for acute/primary CMV infection. All episodes of relapsing viremia occurred independent of acute rejection episodes, augmented immunosuppression or active infections. Additionally, there was no clinical evidence of ganciclovir-resistant CMV in any of the LTR relapsers in this cohort.

CD57 and KLRG1 are rapidly induced in CMV-specific acute CD8^{+} T_{AEFF} (CD27^{+}) during primary infection and undergo phenotypic progression to T_{EM} (CD27^{-}) into chronic infection

We first assessed the dynamics of CD57 and KLRG1 expression, along with other major phenotypic markers, in circulating total CD8^{+} T cell and CMV-specific acute CD8^{+} T_{AEFF} cells in our cohort of D+R-LTRs during acute/primary viremia. We observed increased frequencies of CD57^{+}, KLRG1^{+}, and CD57^{+}CD27^{+} total CD8^{+} T cells during acute/primary CMV infection compared to pre-CMV infection (i.e., before the detection of *de novo* viremia) levels determined in a subset of patients (Fig. 1A–D), along with *de novo* CMV-dextramer responses (Supp. Table I and Supp. Fig. 1B). We next determined CD57

expression in relation to KLRG1 and CD27 expression and found a substantial enrichment of total $CD8^+CD57^+$(Fig 1E and F) and CMV-specific $CD8^+CD57^+$dextramer$^+$ T_{AEFF} cells in the $CD27^+$subset (Fig. 1G and H) during acute infection with evidence of progression to a $CD57^+CD27^-$ predominant subset into chronic infection. Similarly, proportions of $CD57^+KLRG1^+$ cells increased in total $CD8^+$ T cells (Fig 1E and F) and CMV-specific $CD8^+CD57^+KLRG1^+$dextramer$^+$ T_{AEFF}-cells (Fig. 1G and H) from primary into chronic infection. We also assessed other phenotypic markers including CD28, CD38, CD45RA and CD279 (programmed death-1; PD-1) during primary infection and chronic infection. During primary infection, both total and CMV-specific T_{AEFF} predominantly expressed a $CD27^{hi}CD28^{+/-}CD38^+CD279^+CD45RA^-$ acute T effector phenotype (Supp. Fig.1C–F) and progressed to a $CD27^{lo/-}CD28^-CD38^-$ $CD279^-CD45RA^{+/hi}$ T effector memory (T_{EM}) phenotype in chronic infection (Supp. Fig.1E and G). Together, our results demonstrate an unanticipated rapid induction of CMV-specific $CD8^+CD57^+$ T_{AEFF}-cells and $CD8^+KLRG1^+$ T_{AEFF} during acute/primary CMV infection, with a predominant subset of T_{AEFF} that co-express these markers in conjunction with CD27. We then find that these effector populations become progressively enriched into chronic infection, bearing a classical T_{EM} phenotype.

CMV-specific KLRG1$^+$ and CD57$^+$ CD8$^+$ T cells are enriched from primary infection into chronic infection CMV infection and demonstrate in vitro proliferative capacities

We have recently shown the importance of CMV-specific $CD8^+$ T cell proliferation during primary infection for the establishment of immune viral control and up-regulation of the major Type-1 transcription factor, T-bet, in high-risk LTRs (9). Therefore, we next addressed changes in CD57 and KLRG1 expression in CMV-specific $CD8^+$ T cells over the course of CMV infection and determined their relative *in vitro* proliferative capacities during acute and chronic CMV (12 or more months post-primary) in response to CMV peptides. Using an overlapping 15-mer peptide pool of the major CMV antigen, phospho-protein 65 (pp65), we measured *in vitro* CMV-specific proliferation by CFSE dilution at 6 days in 7 LTRs during acute primary CMV infection (Fig. 2A–C). We found that CMV-specific $KLRG1^+CD8^+$ T cells from PBMC proliferated at levels similar to T-bet$^+CD8^+$ T cells (Fig. 2A), while CMV-specific $CD8^+CD57^+$ T cells comprised a significantly reduced population(s) of proliferating cells compared to $KLRG1^+$ and $KLRG1^-$ $CD8^+$ T cells that were $CD57^-$ (Fig. 2A–C). We also tracked CMV-dextramer$^+$ $CD8^+$ T cells *ex vivo* in 3 donors from acute CMV, during the contraction phase (1–2 months after resolution of viremia) and during chronic CMV infection (at least 12 months after primary infection) and found that the majority of CMV dextramer$^+$ cells acquired the $CD57^+KLRG1^+$ phenotype into chronic infection (Fig. 2D). We next wished to assess the *in vitro* proliferative capacities of CMV-dextramer$^+CD8^+$ T cells, however staining was consistently poor for dextramer cells at day 6 following re-stimulation with pooled peptides (data not shown). Therefore, we used the single HLA-restricted dextramer cognate peptides for re-stimulation of PBMC to assess the *in vitro* proliferative capacities at day 6. We previously used this approach to assess CMV-tetramer$^+$ effector responses (9). Using this approach, we assessed the phenotype of proliferating cells during acute (T_{AEFF}) and chronic (T_{EM}) CMV infection in 10 LTRs (Fig. 2E and F). Under these stimulatory conditions $KLRG1^+$, $CD57^+$, and T-bet$^+$ CMV-dextramer$^+$ cells all robustly proliferated, despite the loss of CD27 expression in the majority of cells

progressing from the T_{AEFF} into the T_{EM} stage during chronic CMV infection. Collectively, these data show an enrichment of CMV-specific $CD57^+KLRG1^+CD8^+$ T cells from primary into chronic CMV infection. Further, we find the *in vitro* proliferative capacities of CMV-dextramer$^+$ $KLRG1^+CD8^+$ T cells and $CD57^+CD8^+$ T cells to be robust in response to dextramer cognate CMV peptides, whereas $CD57^+$ cells demonstrated relatively reduced proliferative capacities in response to pooled peptides compared to $CD57^-$ cells, perhaps due to factors such as multiclonal competition and limited antigen concentration.

KLRG1 expression, but not CD57, correlates with CMV-specific $CD8^+$ T_{AEFF} multifunction

A surface phenotypic correlate for effector function has not been well defined in humans. We previously have shown that induction of intracellular T-bet during primary CMV infection in D+R-LTRs highly correlates with CMV-specific $CD8^+$ T cell effector function. Therefore, we next asked whether KLRG1 and/or CD57 surface expression were predictive of CMV-specific $CD8^+$ effector function, compared to T-bet, during acute primary infection (i.e., T_{AEFF}). Using pp65 pooled peptides, we measured *ex vivo* CMV-specific IFN-γ, TNF-α and CD107a expression by flow cytometric intracellular staining (ICS) in a 6 h re-stimulation assay. We found that $KLRG1^+$ expression significantly correlated with CMV-specific IFN-γ, TNF-α and CD107a T_{AEFF} frequencies, similar to T-bet^+ expression in $CD8^+$ T cells (Fig. 3A and B). By comparison, $CD57^+$ expression was an inferior functional correlate for CMV-specific T_{AEFF} r responses and did not reach statistical significance (Fig. 3C). We next assessed CMV-specific $CD8^+$ T_{AEFF} multifunction, i.e., the capacity to produce more than one effector molecule, using Boolean analysis. We found that $KLRG1^+CD8^+$ T_{AEFF} cells demonstrated significantly increased CMV-specific effector multifunction (IFN-γ, TNF-α, and CD107a) compared to KLRG1 $CD8^+$ T_{AEFF} cells (Fig. 3D). Similar findings were observed when we compared T-bet^+ versus T-bet^- CMV-specific effector responses (Fig. 3E). However, in contrast, CMV-specific T_{AEFF} frequencies and multifunction were similar between $CD57^+$ and $CD57^-$ $CD8^+$ T cells (Fig. 3F). Taken together, our data show that KLRG1 expression is a significant functional correlate for both individual and multifunctional CMV-specific $CD8^+$ T_{AEFF} responses, similar to T-bet, whereas CD57 expression is a relatively poor predictor of effector function.

KLRG1 expression correlates with T-bet expression and T-bet associates with the human KLRG1 promoter

Because we found that KLRG1 expression correlated with CMV-specific $CD8^+$ T_{AEFF} function, we then investigated whether there was a relationship between T-bet and KLRG1 in human T cells. An earlier murine study (25) showed that $CD8^+$ T cells from T-$bet^{-/-}$ mice did not express significant surface KLRG1 during LCMV infection, suggesting an important role in regulation. In $CD8^+$ T cells from our cohort, we found a high level of T-bet and KLRG1 co-expression in contrast to CD57 expression (Fig. 4A). Using Spearman rho analysis, we then assessed intracellular T-bet and surface KLRG1 expression and found they were significantly correlated in $CD8^+$ T cells in our cohort during primary CMV infection (Fig. 4B), in contrast to CD57. To further demonstrate a direct association between T-bet and the KLRG1 promoter, we next searched for a putative T-bet binding site within the promoter region of the KLRG1 gene (Supp. Fig. 2A, C), using a consensus T-bet DNA binding matrix and a transcription factor binding site analysis tool (TFBS tools) and identified the T-bet

binding site with the highest TFBS score (13.4) comparable to the well-defined T-bet binding site in the IFN-γ promoter (TFBS score=11.6; data not shown). In contrast, we did not identify putative binding sites within the CD57 promoter (Supp. Fig. 2B). Based on this analysis, we performed a Chromatin Immunoprecipitation assay (ChIP assay) using DNA extracted from PMA/anti-CD3-activated Jurkat T cells, previously shown to have rapid up-regulation of T-bet with activation (36). As shown in Fig. 4C, the pull-down fragment of chromatin containing the KLRG1 promoter proximal to the highest likely putative T-bet binding site, bound T-bet IP chromatin, indicating a direct association between T-bet and KLRG1 promoter. Similarly, the IFN-γ promoter (positive control) bound T-bet IP chromatin, whereas the IL-4 promoter (negative control), GAPDH promoter (housekeeping) or isotype IgG did not bind T-bet IP chromatin. Taken together, our data supports a direct association between T-bet and the KLRG1 promoter, but not the CD57 promoter, in human T cells and supports a role for T-bet in the regulation of KLRG1 gene expression.

D+R− LTR controllers demonstrate increased total and CMV-specific acute/primary KLRG1^{+}CD8^{+} T_{AEFF} than those of LTR relapsers

Having found a direct association between T-bet and KLRG1, we next analyzed KLRG1 surface expression in regard to the capacity for D+R-LTRs to establish durable early viral control in the first 6 months following primary CMV infection. We initially screened 14 patients for all of the cell surface markers we evaluated in Fig. 1 and found that only KLRG1^{+} expression differentiated CMV controllers from relapsers in total CD8^{+}T cells (Fig. 5A). Next, we compared the frequencies of total KLRG1^{+} and CD57^{+}CD8^{+} T cell frequencies versus T-bet^{+}CD8^{+} T cell frequencies in our entire D+R-cohort and found similarly increased levels in controllers for both KLRG1^{+} and T-bet^{+}, but not CD57^{+}CD8^{+}T cell frequencies (Fig. 5B). We then evaluated the frequencies of CMV pp65-specific KLRG1^{+}CD8^{+}T_{AEFF} cells producing IFN-γ, TNF-α or CD107a in our cohort and found significantly increased frequencies of pp65-specific KLRG1^{+}CD8^{+} T_{AEFF} cells producing these effector molecules in LTR controllers compared to relapsers, and similar to T-bet $^{+}$CD8^{+} T_{AEFF} responses (Fig. 5C, D). Last, we assessed CMV dextramer^{+}CD8^{+} T_{AEFF} cells and found significantly increased surface KLRG1^{+} expression differentiated LTR controllers from relapsers compared to other T_{AEFF} surface phenotypic markers (Fig. 5E, F). Collectively, our data demonstrate that acute/primary surface KLRG1^{+}CD8^{+} T_{AEFF} expression is an effector function and phenotypic correlate that differentiates the capacity of $D^{+}R^{-}$ LTRs to establish early immune viral control.

Total and CMV-specific lung mucosal CD8^{+} T_{AEFF} from BAL express reduced levels of KLRG1 and T-bet compared to the blood during acute/primary CMV infection.

In contrast to circulating CD8^{+} T cells, mucosal CD8^{+} resident memory T cells (T_{RM}) were recently reported to express reduced levels of T-bet (37, 38). While we have previously demonstrated high effector function in CMV-specific lung mucosal cells derived from BAL during acute primary CMV infection (13), little is known about KLRG1 and T-bet expression in lung mucosal CMV-specific CD8^{+} T_{AEFF} cells during acute/primary CMV infection. Therefore, we assessed KLRG and T-bet expression lung mucosal versus blood CMV-specific CD8^{+} T_{AEFF} cells during acute primary CMV infection in the context of other key phenotypic markers. As shown in Fig. 6, both total lung CD8 T cells and CMV-specific

$CD8^+$ lung T_{AEFF}-cells express substantially reduced levels of both T-bet and KLRG1 as compared to these cells in the blood. In contrast, CD57 and CD27 were similar in total $CD8^+$ T cells and CMV-specific $CD8^+$ T_{AEFF} cells between these compartments, whereas CD69 and CD103 expression were strikingly increased in the lung compartment. Thus, lung mucosal CMV-specific $CD8^+$ T_{AEFF} cells demonstrated a predominant $KLRG1^{lo}$T-$bet^{lo}CD103^{+/-}CD57^{+/-}CD69^+CD27^+$ phenotype in contrast to systemic CMV-specific $CD8^+$ T_{AEFF} cells which exhibiting a predominant $KLRG1^+$T-$bet^+CD103^-CD57^+CD69^-CD27^+$ phenotype. Together, these data demonstrate significant differences in total and CMV-specific $CD8^+$ T_{AEFF} cells in the lung versus the blood compartments during acute/primary CMV infection.

DISCUSSION

Herein, we demonstrate for the first time that two surface phenotypic markers, CD57 and KLRG1, long associated with terminal T cell differentiation and immunosenescence, are rapidly induced in CMV-specific $CD8^+$ acute effector (T_{AEFF}) cells during primary infection. Our findings provide novel insights into the phenotypic differentiation and function of CMV-specific human $CD8^+$ T cells progressing from the T_{AEFF} to the T_{EM} stage. We show that both $CD57^+$ and $KLRG1^+$ total and CMV $dextramer^+CD8^+$ T_{AEFF} cells are unexpectedly $CD27^{+/hi}$, and progress to the well-described $CD27^-$ phenotype into the memory phase. However, despite co-expression with the immature marker, CD27, our data show that cells which acquire $CD57^+$ demonstrate relatively inferior proliferative capacity following *in vitro* re-stimulation using pp65 15-mer pooled peptides, compared to cells that express KLRG1 alone, or neither marker. These findings suggest an unexpected rapid acquisition of senescence in $CD57^+CD8^+$ T_{AEFF} cells, relative to the expansion capacity of $KLRG1^+CD57^-$ T cells, under conditions of acute viremia and pooled viral antigen exposure. Furthermore, our observed proliferative differences among subsets suggest that the $CD57^-KLRG1^+$ T_{AEFF} population, and likely to a lesser extent, the $CD57^+KLRG1^+$ T_{AEFF} population, give rise to the predominant $CD57^+KLRG1^+$ T_{EM} population over time. Importantly however, we also observed robust intrinsic proliferative capacities in CMV-specific $CD57^+dextramer^+$ T_{AEFF} and T_{EM} cells when re-stimulated *in vitro* with single 8-mer cognate peptides. While this was somewhat unexpected, it further supports the capacity for self-renewal in these cells under more optimal stimulatory conditions (i.e., higher antigen concentration, reduced multiclonal competition that is present following re-stimulation with peptide pool). Notably, we previously reported robust effector responses in response to single cognate peptide in CMV-$tetramer^+$ $CD8^+$ T cells (9). Overall, our findings demonstrate a relative, but not absolute, proliferative defect in $CD8^+CD57^+$ T cells as reported in an earlier study by Brenchley et al. (21). However, there are important experimental differences between these studies, including our assessment of $CD57^+$ T_{AEFF} during primary CMV infection, our use of total PBMC for re-stimulation versus sorted $CD8^+CD57^+$ T cells, and our use of single-peptide re-stimulation to study CMV-specific $dextramer^+$ cells. Conversely, our findings demonstrate substantial proliferative capacities in CMV-specific $CD8^+KLRG1^+$ T_{AEFF} cells unlike previous studies (20) (39) of $CD8^+KLRG1^+$ T cells, albeit with similar experimental differences as highlighted above. Our findings also indicate that the proliferative capacities of CMV-specific $CD8^+KLRG1^+$

T_{AEFF} cells more closely approximates that of CMV-specific $CD8^+$T-bet$^+$ T_{AEFF} cells, with a subset of expanding $KLRG1^+$ T_{AEFF} cells co-expressing CD57. Taken together, our findings demonstrate rapid induction of CD57 and/or KLRG1 in total and CMV-specific $CD8^+$ T_{AEFF} cells with differential proliferative capacities in conjunction with an immature phenotype that progresses to a mature T_{EM} phenotype in chronic CMV infection.

We and others have demonstrated the correlation between T-bet expression and $CD8^+$ effector function playing an important role in CMV, HIV, HBV and HCV immune control (9, 40, 41) (42). We sought to determine whether either CD57 and/or KLRG1 represented a functional immune correlate and found KLRG1 expression in CMV-specific $CD8^+$ T_{AEFF} cells to be a superior immune correlate for IFN-γ, TNF-α and CD107a expression and effector multifunction, similar to T-bet expression, when compared to CD57. Moreover, we compared $KLRG1^+$ and $CD57^+$ surface expression to T-bet$^+$ and found that $KLRG1^+$ frequencies, similar to T-bet$^+$ frequencies, differentiated CMV controller versus relapser clinical phenotypes in our D+R-LTR cohort, as well as effector molecule expression. Importantly, we previously have shown in a similar D+R-LTR cohort, that the frequencies of CMV-specific tetramer$^+$ cells did not differentiate controller versus relapse phenotypes, rather the function of these tetramer$^+$ cells, using single cognate peptide re-stimulation (9). Here, when we compared $KLRG1^+$ and $CD57^+$ frequencies to other surface phenotypic markers expressed in total $CD8^+$ and CMV dextramer$^+$ T_{AEFF} cells, only $KLRG1^+$ expression significantly differentiated the CMV controller versus relapser phenotypes. Collectively, our data point to $KLRG1^+$ surface expression in the blood $CD8^+$ T_{AEFF} pool as a surrogate for T-bet, effector function and the capacity for early CMV control in high-risk D+R-LTRs.

Because we observed a high level of correlation between $KLRG1^+$ and T-bet$^+$ expression in both proliferation and effector function of $CD8^+$ T cells during acute/primary CMV infection, we sought to determine its molecular regulation compared to CD57 (*B3GAT1*). Only the KLRG1 promoter demonstrated high putative binding site scores for T-bet, in contrast to CD57 (*B3GAT1*), and we expectedly found co-precipitation of T-bet and KLRG1 by ChIP assay, similar to IFN-γ, whereas we did not detect any binding to CD57 (*B3GAT1*). While these data support direct regulation of KLRG1 by T-bet, they also highlight a distinct role for CD57 in T cell differentiation. In fact, the precise functional role of CD57, which does not have a counterpart in the mouse, remains incompletely understood. While our studies support CD57 as an early marker of senescence in $CD8^+$ T_{AEFF} cells, alternative functions have been reported. As CD57 is a glycoepitope, several studies have suggested a role for tissue adhesion, including it being a ligand for laminin (43) and L- and P-selectins (44). Thus, CD57 surface expression could mark terminally differentiated cells with broad tissue migratory licensure via cellular adhesion that are important for $CD8^+$ immune surveillance.

Our study provides new insights into the role of KLRG1 expression in CMV-specific T_{AEFF} and T_{EM} cells. Similar to CD57, KLRG1 has been associated with terminal differentiation and immune senescence in human T cells, with the observation of accumulation of $KLRG1^+CD8^+$ T cells with age (27) (45) and prior studies having demonstrated that sorted $KLRG1^+CD8^+$ T cells exhibited replicative senescence in response to mitogen stimulation

(20) (46) (47). KLRG1 has also been shown to be a ligand for the cadherins expressed on epithelial cells, suggesting an important role for effector trafficking, crosstalk and a potential mechanism to limit cytotoxicity (45) (48). Importantly, our studies show that both CMV-specific $CD8^+KLRG1^+$ T_{AEFF} and T_{EM} cells robustly proliferate during acute primary and chronic infection similar to T-bet^+ cells, the transcription factor that binds the KLRG1 promoter, indicating that $KLRG1^+$ expression alone, does not necessarily indicate senescence. However, our studies do support the concept that the acquisition of CD57 co-expression, is associated with cells that demonstrate reduced proliferative capacity in response to CMV pooled peptides. Interestingly, our findings in the human differ from the mouse studies with persistence of KLRG1 expression into the memory phase, though the LCMV infection mouse model used by Joshi et al. was not the chronic LCMV model. Thus, we propose a revised model of human T cell differentiation in the human, where early $KLRG1^+CD57^{+/-}CD27^+$ T_{AEFF} cells more likely reflect the previously described mouse memory precursor effector cells (MPECs) rather than SLECs and establish $KLRG1^+CD57^+CD27^-$ T_{EM} population in the context of chronic CMV infection (Fig 7). We should also point out that, similar to earlier mouse studies, KLRG1 expression marks viral-specific T_{AEFF} cells with potent multifunction, and strongly correlates with the capacity to establish viral control. The correlation of KLRG1 expression with effector function that we observed in peripheral blood T_{AEFF} cells is also consistent with it being a surrogate for T-bet expression. Indeed, our results also show that KLRG1 expression is reduced in lung mucosal $CD8^+$ T_{AEFF} cells expressing lower levels of T-bet, as recently reported in the mouse (49), providing further *ex vivo* evidence of regulation by this transcription factor. Collectively, our data provide new insights into the kinetics of KLRG1 expression, its regulation and the functionality in human T cells in the context of acute primary into chronic CMV infection.

There are several caveats to our study. While our studies focused on T cell responses to pp65, we acknowledge that the total effector response is significantly broader, including $CD4^+$ T cells (50). However, because our earlier study found pp65-specific > IE1-specific $CD8^+$ effector responses during acute primary infection, we focused on pp65 responses (12). We also recognize that our study size is somewhat small, however capturing D+R-LTRs during primary CMV infection and prospectively assessing their clinical phenotype in addition to collecting serial blood samples is challenging. Nonetheless, our study demonstrated statistically significant findings in our study of CD57 and KLRG1 in T_{AEFF} and T_{EM} cells over the course of CMV infection that advances our understanding of T cell differentiation. Future studies will test whether measurement of KLRG1 expression, in particular, is useful to differentiate the capacity for viral control and determining clinical phenotypes in LTRs at high-risk for recurrent CMV infection, which may be useful in guiding clinical antiviral decision-making.

In summary, our study provides new insights into roles of KLRG1 and CD57 in the function and differentiation of human T cells from the T_{AEFF} to the T_{EM} stage during CMV infection. Based on these findings, we propose a revised model for T cell differentiation that incorporates these markers and relates phenotype with function (Fig. 7). We show that rapid induction of KLRG1, but not CD57, in CMV-specific $CD8^+$ T cells differentiates the capacity for effector function and viral control. Further, we provide evidence that KLRG1, but not CD57, is regulated by, and a surrogate for T-bet in human T-broad migratory

capacities via tissue adhesion that are important for $CD8^+$ immune surveillance. Additionally, another study by Cebo et al (51). suggested a potential role for CD57 in IL-6R signaling. Collectively, these alternate functions are consistent with our findings of rapid induction of CD57 during acute primary infection, its similar expression on lung mucosal CMV-specific T_{AEFF} cells compared to the blood, and its progressive enrichment into chronic infection.

Supplementary Material

Refer to Web version on PubMed Central for supplementary material.

Acknowledgement

We thank Drs. Alex Tsankov (Harvard University), Julie Brind' Amour (University of British Columbia), and Tan Jiangning for their technical expertise and assistance in developing ChIP assay. We also thank Drs. Robbie Mailliard, Charles Rinaldo Jr., Olivera Finn (University of Pittsburgh), and Dr. Mark Connors (NIAID) for valuable feedback and discussion of the manuscript.

Funding: This work was supported by National Institute of Health grants R01AI079175 and R01HL133184 (J.F.M.)

Non-standard abbreviations list:

KLRG1	Killer Cell Lectin-like Receptor Subfamily G 1
IPF	Idiopathic Pulmonary Fibrosis
BAL	Bronchoalveolar lavage
LMNC	Lung mononuclear cells
ChIP	Chromatin Immunoprecipitation
LTRs	Lung transplant recipients
T_{AEFF}	Acute effector T cells
T_{EM}	Effector memory T cells
T_{RM}	Resident Memory T cells

REFERENCES:

1. Zamora M 2004 Cytomegalovirus and lung transplantation. Am J Transplant 4: 1219–1226. [PubMed: 15268722]
2. Fishman J 2007 Infection in solid-organ transplant recipients. N Engl J Med 357: 2601–2614. [PubMed: 18094380]
3. Westall G, Michaelides A, Williams T, Snell G, and Kotsimbos T. 2003 Bronchiolitis obliterans syndrome and early human cytomegalovirus DNAaemia dynamics after lung transplantation. Transplantation 75: 2064–2068. [PubMed: 12829913]
4. Kerschner H, Jaksch P, Karigl G, Popow-Kraupp T, Klepetko W, and Puchhammer-Stöckl E. 2009 Cytomegalovirus DNA load patterns developing after lung transplantation are significantly correlated with long-term patient survival. Transplantation 87: 1720–1726. [PubMed: 19502966]

5. Snyder L, Finlen-Copeland C, Turbyfill W, Howell D, Willner D, and Palmer S. 2010 Cytomegalovirus pneumonitis is a risk for bronchiolitis obliterans syndrome in lung transplantation. Am J Respir Crit Care Med 181: 1391–1396. [PubMed: 20167845]
6. Finlen Copeland C, Davis W, Snyder L, Banks M, Avery R, Davis R, and Palmer S. 2011 Long-term efficacy and safety of 12 months of valganciclovir prophylaxis compared with 3 months after lung transplantation: a single-center, long-term follow-up analysis from a randomized, controlled cytomegalovirus prevention trial. J Heart Lung Transplant 30: 990–996. [PubMed: 21489817]
7. Yusen R, Edwards L, Dipchand A, Goldfarb S, Kucheryavaya A, Levvey B, Lund L, Meiser B, Rossano J, Stehlik J, and S. f. H. a. L. T. International. 2016 The Registry of the International Society for Heart and Lung Transplantation: Thirty-third Adult Lung and Heart-Lung Transplant Report-2016; Focus Theme: Primary Diagnostic Indications for Transplant. J Heart Lung Transplant 35: 1170–1184. [PubMed: 27772669]
8. Pipeling M, John E, Orens J, Lechtzin N, and McDyer J. 2011 Primary cytomegalovirus phosphoprotein 65-specific CD8+ T-cell responses and T-bet levels predict immune control during early chronic infection in lung transplant recipients. J Infect Dis 204: 1663–1671. [PubMed: 22021622]
9. Popescu I, Pipeling M, Shah P, Orens J, and McDyer J. 2014 T-bet:Eomes balance, effector function, and proliferation of cytomegalovirus-specific CD8+ T cells during primary infection differentiates the capacity for durable immune control. J Immunol 193: 5709–5722. [PubMed: 25339676]
10. Popescu I, Pipeling M, Mannem H, Shah P, Orens J, Connors M, Migueles S, and McDyer J. 2016 IL-12-Dependent Cytomegalovirus-Specific CD4+ T Cell Proliferation, T-bet Induction, and Effector Multifunction during Primary Infection Are Key Determinants for Early Immune Control. J Immunol 196: 877–890. [PubMed: 26663780]
11. Popescu I, Mannem H, Winters S, Hoji A, Silveira F, McNally E, Pipeling M, Lendermon E, Morrell M, Pilewski J, Hanumanthu V, Zhang Y, Gulati S, Shah P, Iasella C, Ensor C, Armanios M, and McDyer J. 2018 Impaired CMV Immunity in Idiopathic Pulmonary Fibrosis Lung Transplant Recipients with Short Telomeres. Am J Respir Crit Care Med.
12. Pipeling M, West E, Osborne C, Whitlock A, Dropulic L, Willett M, Forman M, Valsamakis A, Orens J, Moller D, Lechtzin N, Migueles S, Connors M, and McDyer J. 2008 Differential CMV-specific CD8+ effector T cell responses in the lung allograft predominate over the blood during human primary infection. J Immunol 181: 546–556. [PubMed: 18566421]
13. Akulian J, Pipeling M, John E, Orens J, Lechtzin N, and McDyer J. 2013 High-quality CMV-specific CD4+ memory is enriched in the lung allograft and is associated with mucosal viral control. Am J Transplant 13: 146–156. [PubMed: 23016698]
14. Wherry EJ, Teichgraber V, Becker TC, Masopust D, Kaech SM, Antia R, von Andrian UH, and Ahmed R. 2003 Lineage relationship and protective immunity of memory CD8 T cell subsets. Nat Immunol 4: 225–234. [PubMed: 12563257]
15. Seder RA, and Ahmed R. 2003 Similarities and differences in CD4+ and CD8+ effector and memory T cell generation. Nat Immunol 4: 835–842. [PubMed: 12942084]
16. Appay V, van Lier R, Sallusto F, and Roederer M. 2008 Phenotype and function of human T lymphocyte subsets: consensus and issues. Cytometry A 73: 975–983. [PubMed: 18785267]
17. Hamann D, Baars P, Rep M, Hooibrink B, Kerkhof-Garde S, Klein M, and van Lier R. 1997 Phenotypic and functional separation of memory and effector human CD8+ T cells. J Exp Med 186: 1407–1418. [PubMed: 9348298]
18. De Rosa SC, Herzenberg LA, and Roederer M. 2001 11-color, 13-parameter flow cytometry: Identification of human naive T cells by phenotype, function, and T-cell receptor diversity. Nat Med 7: 245–248. [PubMed: 11175858]
19. Appay V, Dunbar PR, Callan M, Klenerman P, Gillespie GM, Papagno L, Ogg GS, King A, Lechner F, Spina CA, Little S, Havlir DV, Richman DD, Gruener N, Pape G, Waters A, Easterbrook P, Salio M, Cerundolo V, McMichael AJ, and Rowland-Jones SL. 2002 Memory CD8+ T cells vary in differentiation phenotype in different persistent virus infections. Nat Med 8: 379–385. [PubMed: 11927944]
20. Voehringer D, Koschella M, and Pircher H. 2002 Lack of proliferative capacity of human effector and memory T cells expressing killer cell lectin-like receptor G1 (KLRG1). Blood 100: 3698–3702. [PubMed: 12393723]

21. Brenchley JM, Karandikar NJ, Betts MR, Ambrozak DR, Hill BJ, Crotty LE, Casazza JP, Kuruppu J, Migueles SA, Connors M, Roederer M, Douek DC, and Koup RA. 2003 Expression of CD57 defines replicative senescence and antigen-induced apoptotic death of CD8+ T cells. Blood 101: 2711–2720. [PubMed: 12433688]
22. Papagno L, Spina CA, Marchant A, Salio M, Rufer N, Little S, Dong T, Chesney G, Waters A, Easterbrook P, Dunbar PR, Shepherd D, Cerundolo V, Emery V, Griffiths P, Conlon C, McMichael AJ, Richman DD, Rowland-Jones SL, and Appay V. 2004 Immune activation and CD8+ T-cell differentiation towards senescence in HIV-1 infection. PLoS Biol 2: E20. [PubMed: 14966528]
23. Hoji A, Connolly N, Buchanan W, and Rinaldo CJ. 2007 CD27 and CD57 expression reveals atypical differentiation of human immunodeficiency virus type 1-specific memory CD8+ T cells. Clin Vaccine Immunol 14: 74–80. [PubMed: 17079436]
24. Gamadia LE, van Leeuwen EM, Remmerswaal EB, Yong SL, Surachno S, Wertheim-van Dillen PM, Ten Berge IJ, and Van Lier RA. 2004 The size and phenotype of virus-specific T cell populations is determined by repetitive antigenic stimulation and environmental cytokines. J Immunol 172: 6107–6114. [PubMed: 15128796]
25. Joshi N, Cui W, Chandele A, Lee H, Urso D, Hagman J, Gapin L, and Kaech S. 2007 Inflammation directs memory precursor and short-lived effector CD8(+) T cell fates via the graded expression of T-bet transcription factor. Immunity 27: 281–295. [PubMed: 17723218]
26. Dolfi D, Mansfield K, Polley A, Doyle S, Freeman G, Pircher H, Schmader K, and Wherry E. 2013 Increased T-bet is associated with senescence of influenza virus-specific CD8 T cells in aged humans. J Leukoc Biol 93: 825–836. [PubMed: 23440501]
27. Ouyang Q, Wagner W, Voehringer D, Wikby A, Klatt T, Walter S, Müller C, Pircher H, and Pawelec G. 2003 Age-associated accumulation of CMV-specific CD8+ T cells expressing the inhibitory killer cell lectin-like receptor G1 (KLRG1). Exp Gerontol 38: 911–920. [PubMed: 12915213]
28. Ibegbu C, Xu Y, Harris W, Maggio D, Miller J, and Kourtis A. 2005 Expression of killer cell lectin-like receptor G1 on antigen-specific human CD8+ T lymphocytes during active, latent, and resolved infection and its relation with CD57. J Immunol 174: 6088–6094. [PubMed: 15879103]
29. Roederer M, Nozzi J, and Nason M. 2011 SPICE: Exploration and analysis of post-cytometric complex multivariate datasets. Cytometry A.
30. Brind'Amour J, Liu S, Hudson M, Chen C, Karimi M, and Lorincz M. 2015 An ultra-low-input native ChIP-seq protocol for genome-wide profiling of rare cell populations. Nat Commun 6: 6033. [PubMed: 25607992]
31. Tsankov A, Gu H, Akopian V, Ziller M, Donaghey J, Amit I, Gnirke A, and Meissner A. 2015 Transcription factor binding dynamics during human ES cell differentiation. Nature 518: 344–349. [PubMed: 25693565]
32. Ye J, Coulouris G, Zaretskaya I, Cutcutache I, Rozen S, and Madden TL. 2012 Primer-BLAST: a tool to design target-specific primers for polymerase chain reaction. BMC Bioinformatics 13: 134. [PubMed: 22708584]
33. Zhou X, Jiang Y, Lu L, Ding Q, Jiao Z, Zhou Y, Xin L, and Chou KY. 2007 MHC class II transactivator represses human IL-4 gene transcription by interruption of promoter binding with CBP/p300, STAT6 and NFAT1 via histone hypoacetylation. Immunology 122: 476–485. [PubMed: 17645498]
34. Tan G, and Lenhard B. 2016 TFBSTools: an R/bioconductor package for transcription factor binding site analysis. Bioinformatics 32: 1555–1556. [PubMed: 26794315]
35. Tan G 2017 JASPAR2018: Data package for JASPAR 2018..
36. Beima KM, Miazgowicz MM, Lewis MD, Yan PS, Huang TH, and Weinmann AS. 2006 T-bet binding to newly identified target gene promoters is cell type-independent but results in variable context-dependent functional effects. The Journal of biological chemistry 281: 11992–12000. [PubMed: 16473879]
37. Hombrink P, Helbig C, Backer RA, Piet B, Oja AE, Stark R, Brasser G, Jongejan A, Jonkers RE, Nota B, Basak O, Clevers HC, Moerland PD, Amsen D, and van Lier RA. 2016 Programs for the persistence, vigilance and control of human CD8(+) lung-resident memory T cells. Nature immunology 17: 1467–1478. [PubMed: 27776108]

38. Mueller SN, and Mackay LK. 2016 Tissue-resident memory T cells: local specialists in immune defence. Nature reviews. Immunology 16: 79–89.
39. Bengsch B, Spangenberg H, Kersting N, Neumann-Haefelin C, Panther E, von Weizsäcker F, Blum H, Pircher H, and Thimme R. 2007 Analysis of CD127 and KLRG1 expression on hepatitis C virus-specific CD8+ T cells reveals the existence of different memory T-cell subsets in the peripheral blood and liver. J Virol 81: 945–953. [PubMed: 17079288]
40. Hersperger A, Martin J, Shin L, Sheth P, Kovacs C, Cosma G, Makedonas G, Pereyra F, Walker B, Kaul R, Deeks S, and Betts M. 2011 Increased HIV-specific CD8+ T-cell cytotoxic potential in HIV elite controllers is associated with T-bet expression. Blood 117: 3799–3808. [PubMed: 21289310]
41. Kurktschiev P, Raziorrouh B, Schraut W, Backmund M, Wächtler M, Wendtner C, Bengsch B, Thimme R, Denk G, Zachoval R, Dick A, Spannagl M, Haas J, Diepolder H, Jung M, and Gruener N. 2014 Dysfunctional CD8+ T cells in hepatitis B and C are characterized by a lack of antigen-specific T-bet induction. J Exp Med 211: 2047–2059. [PubMed: 25225458]
42. Barnett B, Staupe R, Odorizzi P, Palko O, Tomov V, Mahan A, Gunn B, Chen D, Paley M, Alter G, Reiner S, Lauer G, Teijaro J, and Wherry E. 2016 Cutting Edge: B Cell-Intrinsic T-bet Expression Is Required To Control Chronic Viral Infection. J Immunol 197: 1017–1022. [PubMed: 27430722]
43. Kizuka Y, Kobayashi K, Kakuda S, Nakajima Y, Itoh S, Kawasaki N, and Oka S. 2008 Laminin-1 is a novel carrier glycoprotein for the nonsulfated HNK-1 epitope in mouse kidney. Glycobiology 18: 331–338. [PubMed: 18263654]
44. Needham L, and Schnaar R. 1993 The HNK-1 reactive sulfoglucuronyl glycolipids are ligands for L-selectin and P-selectin but not E-selectin. Proc Natl Acad Sci U S A 90: 1359–1363. [PubMed: 7679503]
45. Ito M, Maruyama T, Saito N, Koganei S, Yamamoto K, and Matsumoto N. 2006 Killer cell lectin-like receptor G1 binds three members of the classical cadherin family to inhibit NK cell cytotoxicity. J Exp Med 203: 289–295. [PubMed: 16461340]
46. Thimme R, Appay V, Koschella M, Panther E, Roth E, Hislop A, Rickinson A, Rowland-Jones S, Blum H, and Pircher H. 2005 Increased expression of the NK cell receptor KLRG1 by virus-specific CD8 T cells during persistent antigen stimulation. J Virol 79: 12112–12116. [PubMed: 16140789]
47. Henson S, Franzese O, Macaulay R, Libri V, Azevedo R, Kiani-Alikhan S, Plunkett F, Masters J, Jackson S, Griffiths S, Pircher H, Soares M, and Akbar A. 2009 KLRG1 signaling induces defective Akt (ser473) phosphorylation and proliferative dysfunction of highly differentiated CD8+ T cells. Blood 113: 6619–6628. [PubMed: 19406987]
48. Tessmer M, Fugere C, Stevenaert F, Naidenko O, Chong H, Leclercq G, and Brossay L. 2007 KLRG1 binds cadherins and preferentially associates with SHIP-1. Int Immunol 19: 391–400. [PubMed: 17307799]
49. Sheridan B, Pham Q, Lee Y, Cauley L, Puddington L, and Lefrançois L. 2014 Oral infection drives a distinct population of intestinal resident memory CD8(+) T cells with enhanced protective function. Immunity 40: 747–757. [PubMed: 24792910]
50. Sylwester A, Mitchell B, Edgar J, Taormina C, Pelte C, Ruchti F, Sleath P, Grabstein K, Hosken N, Kern F, Nelson J, and Picker L. 2005 Broadly targeted human cytomegalovirus-specific CD4+ and CD8+ T cells dominate the memory compartments of exposed subjects. J Exp Med 202: 673–685. [PubMed: 16147978]
51. Cebo C, Durier V, Lagant P, Maes E, Florea D, Lefebvre T, Strecker G, Vergoten G, and Zanetta JP. 2002 Function and molecular modeling of the interaction between human interleukin 6 and its HNK-1 oligosaccharide ligands. J Biol Chem 277: 12246–12252. [PubMed: 11788581]

KEY POINTS

- We report novel CMV-specific KLRG1^{+}CD27^{+}CD57$^{+/-}$ CD8^{+} T_{AEFF} in primary infection.
- KLRG1^{+} T_{AEFF} correlates with CMV function and control in lung transplant patients.

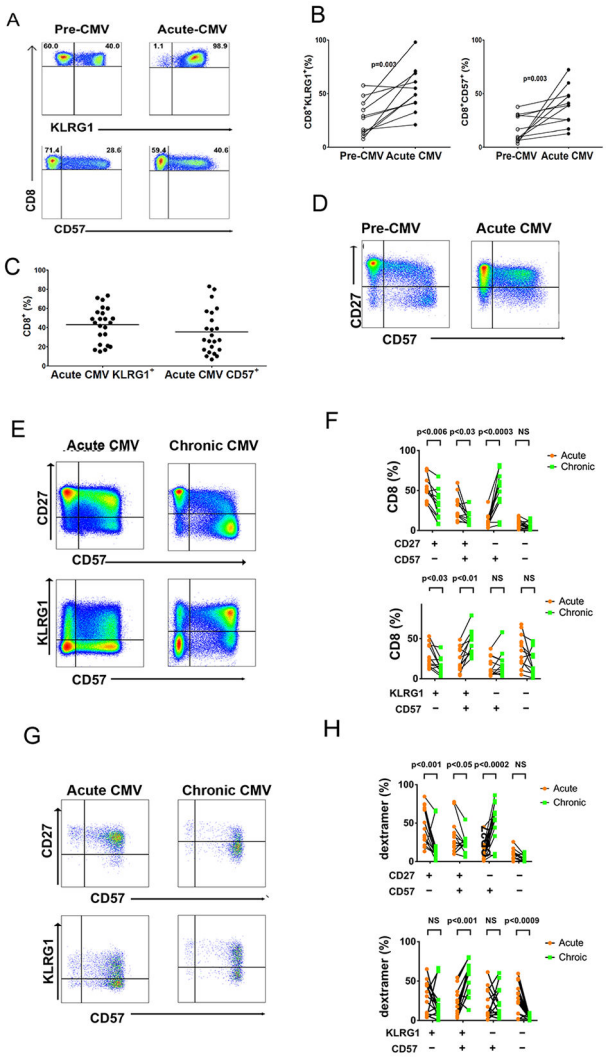

Figure 1. Rapid Induction of KLRG1$^+$ and CD57$^+$ surface expression in CMV specific CD8 T_{AEFF} during acute primary CMV infection evolve into T_{EM} during chronic infection.

(A) Representative flow cytometric plots show the expression of KLRG1$^+$ *(upper panel)* and CD57$^+$ *(lower panel)* in total CD8$^+$ T cells from D+R-patient during Pre-CMV and Acute CMV infection. Total CD8$^+$ T cells were gated on live CD3$^+$ T cells after excluding CD14$^+$, CD16$^+$, and CD19$^+$ cells. (B) Cumulative data showing distributions of total KLRG1$^+$CD8$^+$ (*left graph*) and CD57$^+$CD8$^+$ (*right graph*) T cells from patients during Pre-CMV and Acute CMV infection (n=8). Statistical analysis was performed using Wilcoxon matched pair signed rank test. Also Mann-Whitney U test was performed with a two-sided and p value of less than 0.05 considered statistically significant. (C) Cumulative data shows distributions of total CD3$^+$CD8$^+$ T cells KLRG1$^+$ and CD57$^+$ for (n=23) patients during Acute CMV) infection. (D) Representative flow cytometric plots show expression of CD57$^+$ and CD27$^+$ on CD8$^+$ T cells during Pre-CMV (*left plot*) and Acute CMV (*right plot*). (E) Representative flow cytometric plots showing co-expression of CD57$^+$ and CD27$^+$ *(upper panels)* or KLRG1$^+$ and CD57$^+$ *(lower panels)* on the gated population of total CD3$^+$CD8$^+$ T cells *ex vivo* from D+R-patient during Acute CMV (*left plots*) and Chronic CMV (*right plots*)

infection. (F) Cumulative data graph showing frequency of total $CD8^+$ T cells expressing phenotypic markers as labeled. PBMCs from acute CMV *(orange circles)* and chronic CMV *(green squares)* (n=14 dextramer responses) D+R-patients were stained *ex vivo* and analyzed by flow cytometry. (G) Representative plots show $CD57^+$ and $KLRG1^+$ expression on MHC class I dextramer cells and co-expression of $CD57^+$, and $CD27^+$ or $KLRG1^+$ on the gated population $dextramer^+$ cells $CD3^+CD8^+$ T cells. (H) Cumulative data graph shows proportions of total $CD8^+$ T cells proportions of MHC class I $dextramer^+$ cells from acute CMV (n=14 dextramer responses) *(orange circles)* and chronic CMV (n=14 dextramer responses) *(green squares)* infection, expressing distinct phenotypic markers are shown.

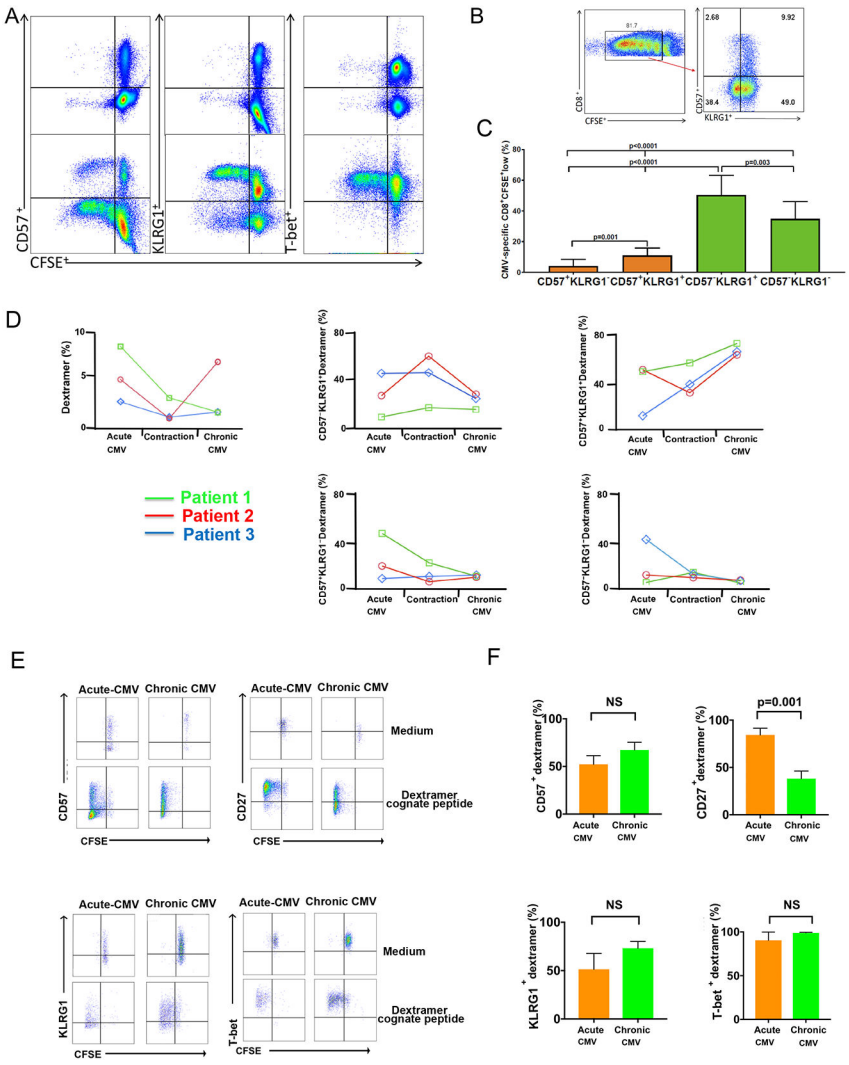

Figure 2. Phenotype and proliferation of CD57$^+$ and/or KLRG1$^+$ CMV-specific CD8$^+$ T cells from primary into chronic CMV infection.

(A) Representative flow cytometry plots from the Acute CMV showing phenotype and CMV pp65-specific proliferation in response to pp65 pooled peptides *(lower panels)* or medium alone (negative control) (*upper panels*), KLRG1$^+$ (*middle panels*) and T-bet$^+$ (*right panels*). (B) Representative flow plot from (A) showing KLRG1$^{+/-}$ and CD57$^{+/-}$ phenotypes in CD8$^+$CFSE^{lo} subset (*right panel*). (C) Cumulative data showing CMV pp65-specific proliferation at 6 days for CD8$^+$ T cells with respect to CD57$^+$ *(orange bars)*, CD57$^-$ *(green bars)* of CFSE^{lo} events (n=7). Bars represent median values of CFSE^{lo} events for CD57$^+$KLRG1$^-$, CD57$^+$KLRG1$^+$, CD57$^-$KLRG1$^+$ and CD57$^-$KLRG1$^-$ respectively. Statistical analysis performed using Mann-Whitney U test with a two-sided and p value of less than 0.05 considered statistically significant. (D) Graphs showing frequencies of CMV-dextramer CD8$^+$ T cells, and KLRG1$^{+/-}$ CD57$^{+/-}$ subsets in three patients during Acute-CMV, Contraction phase, and Chronic CMV infection. Samples for the contraction phase were obtained 1–2 months following clearance of acute viremia and Chronic CMV at least a year post-Acute CMV. (E) Representative flow cytometry plots of CMV dextramer

proliferation in response to cognate peptide re-stimulation or medium measured at 6 days using CFSE dilution. Shown are responses during Acute-CMV and Chronic CMV and phenotypic markers $CD57^+$ *(upper left*), $CD27^+$ (u*pper right*), $KLRG1^+$ *(lower left)* and T-bet^+ (*lower right*) plots. (F) Cumulative data from (E) showing respective phenotypes of $CFSE^{lo}$ events in $dextramer^+$ cells. during Acute-CMV *(orange bars)* and Chronic CMV *(green bars)*. Bars represent median values of $CFSE^{lo}$ frequencies. Statistical analysis performed using Mann-Whitney U test with a two-sided and p value of less than 0.05 considered statistically significant. NS=non-significant.

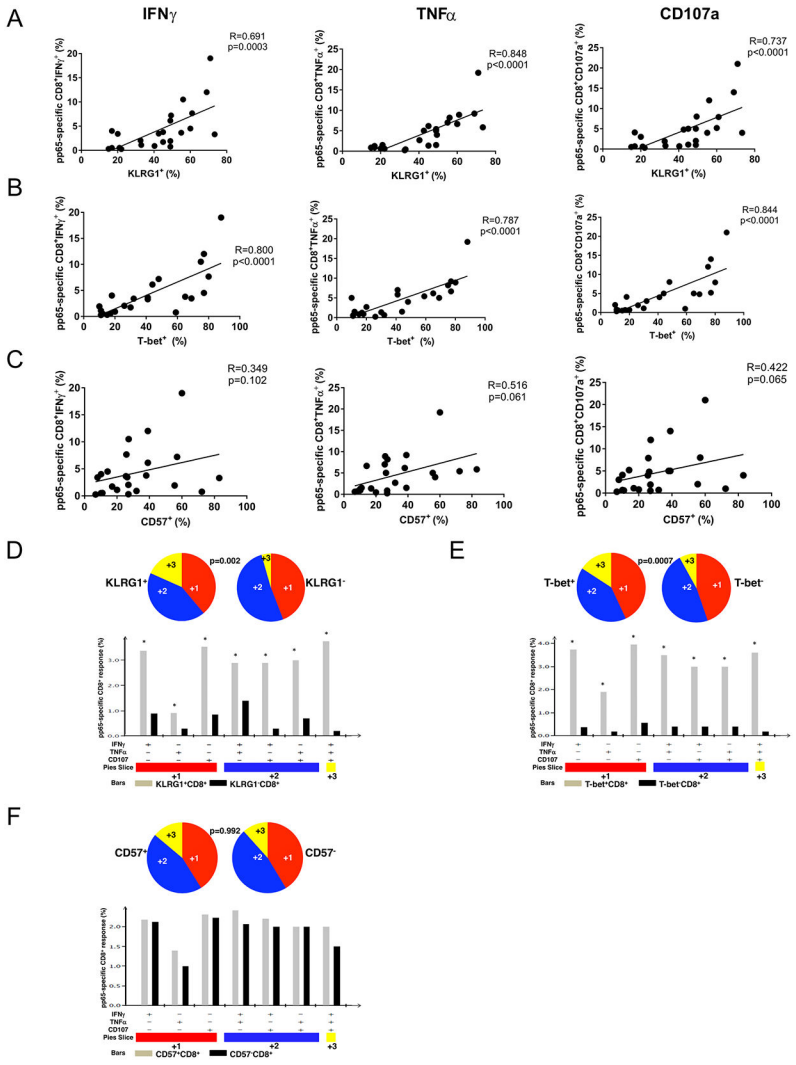

Figure 3. CMV pp65-specific CD8$^+$ effector responses reciprocally correlate with T-bet and KLRG1 expression but not with CD57 and CD8$^+$KLRG1$^+$ effectors have higher quantity and quality of multifunction during acute primary CMV infection similar to CD8$^+$T-bet$^+$ effectors.

(A) Cumulative correlation data (n=23) by scatter plot analysis of KLRG1$^+$, T-bet$^+$ (B) and CD57$^+$ (C), frequencies and CMV-specific pp65 frequencies for CD8$^+$IFNγ$^+$ *(left panels)*, tumor necrosis factor (TNFα) CD8$^+$TNFα *(middle panels)* and CD8$^+$CD107a$^+$ *(right panels)* during acute CMV infection from the LTR cohort. Correlation coefficient (R) and p values were calculated using Spearman rank correlation test. (D) Individual pie charts of PBMC reflecting CD8$^+$KLRG1$^+$ *(left pie)* and CD8$^+$KLRG1$^-$ *(right pie)* of T cell effector multifunction (E) CD8$^+$T-bet$^+$ *(left pie)* and CD8$^+$T-bet$^-$ *(right pie)* of CMV pp65–specific T cell effector multifunction and (F) CD8$^+$CD57$^+$ *(left pie)* and CD8$^+$CD57$^-$ *(right pie)* of CMV pp65–specific T cell during acute primary CMV infection responses (IFN-γ, TNF-α, CD107a) from the LTR cohort effector multifunction. Using Boolean analysis, the percentage of total and individual effector multifunctional subset responses for CD8$^+$ T cells from KLRG1$^+$ *(gray bars)* and KLRG1$^-$ *(black bars)* or T-bet$^+$ *(gray bars)* and T-bet$^-$ *(black bars)* or CD57$^+$ *(gray bars)* and CD57$^-$ *(black bars)* are shown in the bar graph for each of the multifunctional subsets. * p<0.05. *Significant differences when comparing mean

frequencies of single and multifunctional responses, p less than or equal to 0.05. All pvalues were determined by the Kruskal-Wallis one-way ANOVA or Wilcoxon signed rank test. Data analyzed using the program SPICE.

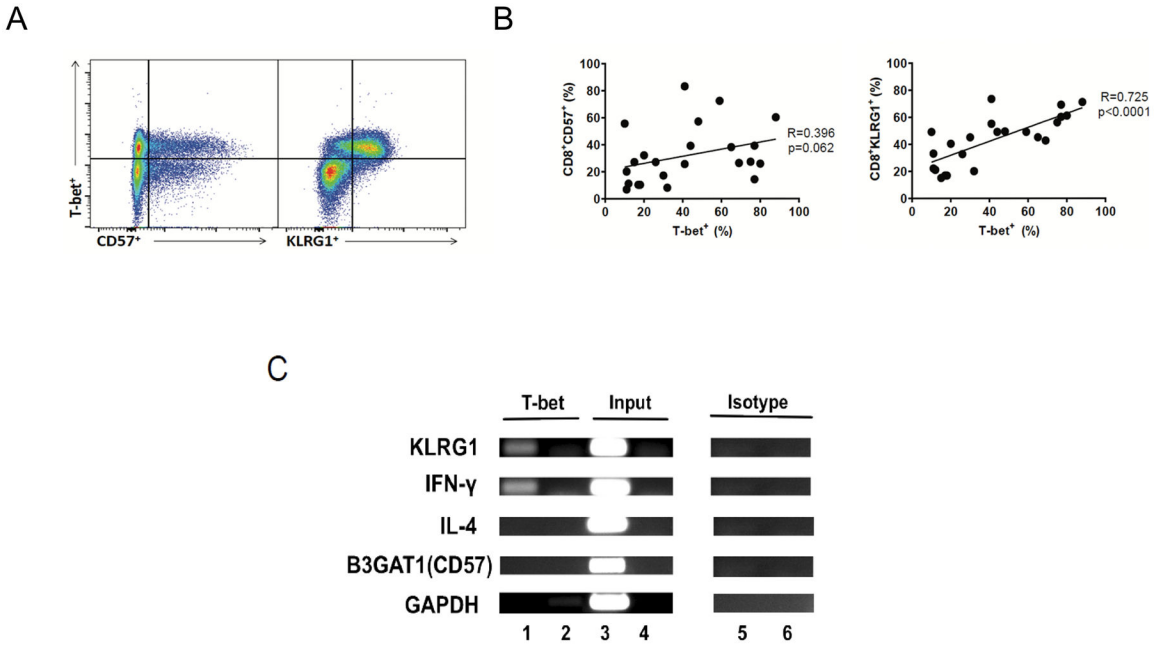

Figure 4. T-bet expression significantly correlates with KLRG1 in CD8$^+$ T cells during primary CMV infection and T-bet interacts with the KLRG1 promoter in human T cells.

(A) Representative flow cytometric plots showing co-expression of T-bet$^+$ and KLRG1$^+$ or CD57$^+$ gated on live CD3$^+$CD8$^+$ T cells. This is a representative of n=23 individuals. (B) Cumulative correlation data (n=23) by scatter plot analysis of T-bet$^+$ and CD8$^+$CD57$^+$ *(left panel)*, and CD8$^+$KLRG1$^+$ *(right panel)*, frequencies during acute CMV infection from the LTR cohort. A black line indicates the regression line as well as R and p value that were generated using the Spearman's Rank Correlation test. (C) Agarose gel images showing bands of semi-quantitative PCR amplicons that reside in the promoter sequence of T-bet targets, KLRG1, CD57 (*B3GAT1*) and IFN-γ (positive control) as performed by ChIP assay. Also shown are non T-bet targets, IL-4 (negative control), and GAPDH (negative control) genes. ChIP assay was performed using human Jurkat T cell line using mouse anti-human TBX21 antibody (clone 39D; IgG1). Immnunoprecipitated DNA was subject to PCR amplification using primer sets for KLRG1, CD57(*B3GAT1*), IFN-γ, IL-4, and GAPDH targets (lane 1) for each corresponding region of promoter sequences in proximity to the T-bet binding site for each gene. Results of PCR amplifications of input DNA (lane 3) or mouse IgG1 isotype control antibody (lane 5) are also shown. Lanes 2, 4, and 6 show non-template PCR negative controls.

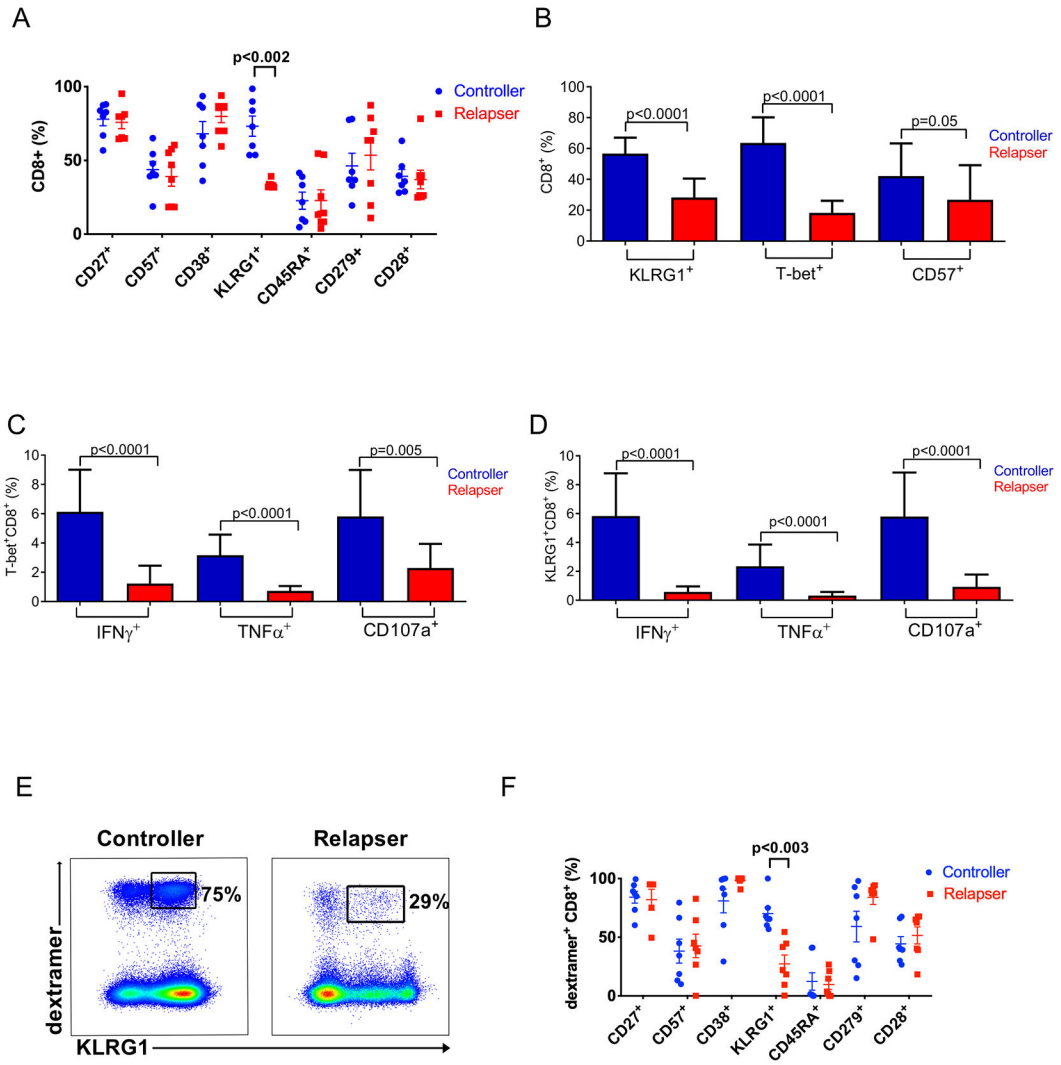

Figure 5. Significantly higher frequencies of KLRG1$^+$ total CD8$^+$ and CMV-specific CD8$^+$ T cells are found in viremic controllers compared to relapsers.

(A) Cumulative distributions of KLRG1 frequency and additional six phenotypic markers expressed on the total CD8$^+$ T cell among controllers *(blue circles)* (n=7) and the relapsers *(red squares)* (n=8) are shown (mean ± SEM). Only the KLRG1 expression exhibits the significant difference ($p<0.002$) between controllers and relapser as indicated. (B) Cumulative data shows frequency of KLRG1$^+$, T-bet$^+$, or CD57$^+$ total CD8$^+$ T cells among controllers *(blue columns)* (n=13) and relapsers *(red columns)* (n=10). (C) Cumulative data shows Tbet$^+$CD8$^+$ frequencies and (D) KLRG1$^+$CD8$^+$effector functions (IFN-γ$^+$, TNF-α$^+$, CD107a$^+$) in controllers *(blue columns)* and relapsers *(red columns)*. (E) Representative flow cytometric plot shows KLRG1$^+$ expression on CMV-specific dextramer$^+$CD8$^+$ T cells. Numbers show proportion of KLRG1$^+$ subset within the gated dextramer$^+$CD8$^+$ T cell in a controller *(left panel)* versus a relapser *(right panel)*. (F) Cumulative distributions of KLRG1$^+$ frequency and additional six phenotypic markers expressed on the Dextramer $^+$CD8$^+$ T cell among controllers *(blue circles)* (n=8 dextramer responses assed) and the relapsers *(red squares)* (n=7 dextramer responses assed) are shown (mean ± SEM).

Statistical analysis performed using Mann-Whitney U test with a two-sided and p value of less than 0.05 considered statistically significant between the controller and the relapser throughout the course of statistical analyses. NS=non-significant.

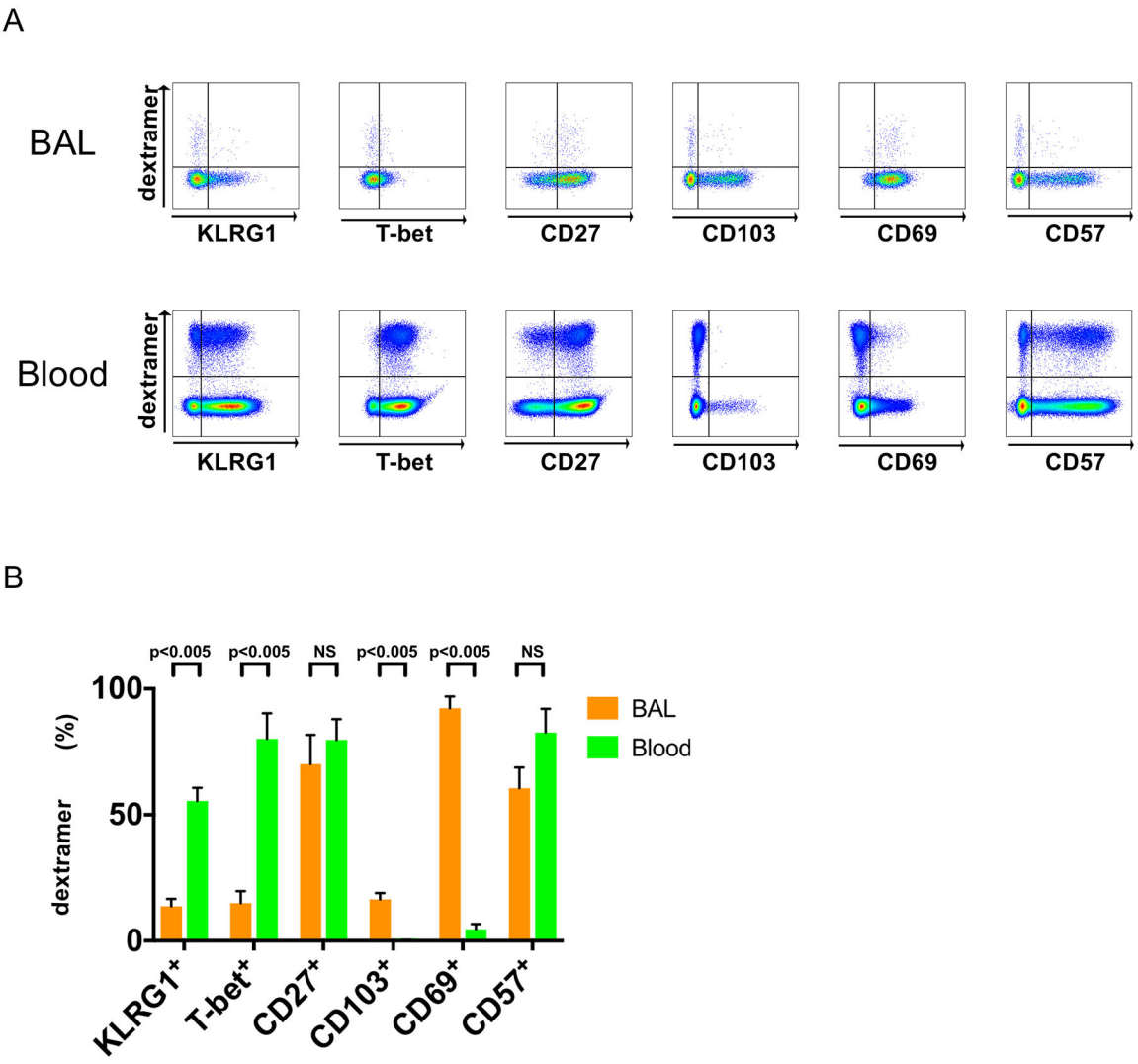

Figure 6. CMV-specific Dextramer^{+}CD8^{+} T cells in BAL express lower levels of KLRG1 and T-bet transcription factor than PBMC.

(A**)** Representative flow cytometry plots of CMV dextramer^{+}CD8^{+} Tcells BAL cells *(upper panels)* and Blood *(lower panels)* during acute/primary CMV infection (n=6) for a panel of six markers: KLRG1^{+}, T-bet^{+}, CD27^{+}, CD103^{+}, CD69^{+} and CD57^{+} plots. (B) A cumulative data of summary of phenotypic frequency analysis of (A) showing BAL cells *(orange bars)* and PBMC *(green bars).* Statistical analysis performed using Mann-Whitney U test with a two-sided and p value of less than 0.05 considered statistically significant between the BAL and Blood compartments. NS=non-significant.

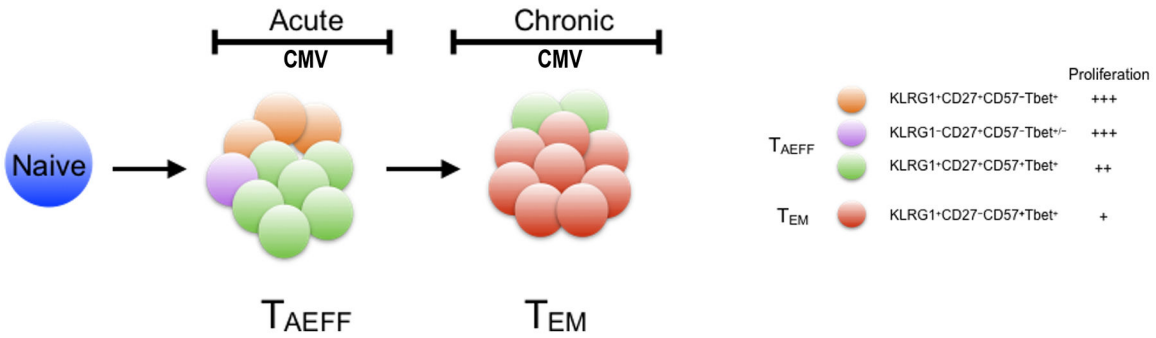

Figure 7. CMV-specific CD8$^+$ T effector cell differentiation model.

A figure depicts our simplified linear model of the CMV-specific CD8$^+$ effector T cell differentiation. According to the model, antigen primed CMV-specific CD8$^+$ naive T cells *(blue circle)* undergo extensive clonal expansion and concurrent effector differentiation upon viral antigen encounter during CMV primary/acute viremia. An expanded pool of T_{AEFF} subsets, including a predominant KLRG1$^+$CD27$^+$CD57$^+$T-bet$^+$ subset *(green circle)* are generated. T_{AEFF}, particularly KLRG1$^+$ T_{AEFF} is central to the anti-viral cell immunity during primary/acute infection and the subsequent formation of KLRG1$^+$CD27$^-$CD57$^+$ T_{EM} *(red circle)* in the chronic phase. These T_{AEFF}, despite expressing two effector markers, KLRG1 and CD57, exibit differential proliferative capacities *(middle panel)* with increasing expression of KLRG1 and CD57, and declining expression of CD27 over the course of T_{EM} differentiation. Although each phases of infection is represented by a few dominant subsets, in reality such stages likely made up of multiple subsets albeit low frequencies.

Table I.

Patient characteristics and clinical phenotypes following primary CMV infection in D+R-LTRs.

LTR	Age (y)	Gender	Primary Diagnosis	Immunosuppression at Primary CMV Onset	Primary CMV Onset[a]	Relapsing Viremia
23	50	M	Idiopathic Pulmonary Fibrosis	CSA 175/100, RAPA 1^1,Pred 5^1	108	-
24	31	F	Cystic Fibrosis	TAC 1.5^2, MMF 0.5^2,Pred 10^1	96	+
25	34	F	Primary Pulmonary Hypertension	TAC 4^2, MMF 0.5^2,Pred 10^1	129	-
28	33	F	Cystic Fibrosis	TAC 6^2, MMF 0.5^2,Pred 10^1	210	-
29	62	F	COPD	TAC 2.5^2, MMF 0.5^2,Pred 10^1	168	+
31	55	M	Cystic Fibrosis	TAC 3^2, AZA 50^1,Pred 5^1	248	-
33	51	F	Idiopathic Pulmonary Fibrosis	TAC 2^2, MMF 0.5^3,Pred 7.5^1	186	+
34	59	F	COPD	TAC 4^2, MMF 0.25^2,Pred 10^1	174	-
35	27	M	Cystic Fibrosis	TAC 1^2, MMF 0.5^2,Pred 7.5^1	219	-
36	49	F	Idiopathic Pulmonary Fibrosis	TAC 4^2, MMF 0.25^2,Pred 10^1	167	+
37	56	F	Obliterative Bronchiolitis	TAC 5^2, MMF 0.5^4,Pred 10^1	133	-
38	56	M	COPD	TAC 1^2, MMF 1^2,Pred 10^1	155	-
40	54	F	COPD	TAC 1.5^2, MMF 0.5^4,Pred 15^1	122	-
41	64	F	Bronchiectasis	TAC 4^2, MMF 0.5^2,Pred 5^1	184	-
43	51	M	Sarcoidosis	TAC 4^2, MMF 0.5^2,Pred 15^1	83	+
45	21	M	Cystic Fibrosis	TAC 2.5^2, MMF 0.5^3,Pred 15^1	92	-
46	59	M	COPD	TAC 1.5^2, MMF 1^2,Pred 20^1	37	+
48	47	M	Idiopathic Pulmonary Fibrosis	TAC 2^2, MMF 0.25^2,Pred 10^1	162	+
51	41	F	Pulmonary Hypertension	TAC 2^2, MMF 0.5^2,Pred 7.5^1	214	-
53	35	F	Cystic Fibrosis	TAC 2^2, MMF 0.5^2,Pred 10^1	125	+
56	61	F	COPD	TAC 1^2, MMF 0.5^2,Pred 10^1	142	+
57	56	M	Idiopathic Pulmonary Fibrosis	TAC 2^2, MMF 0.25^2,Pred 10^1	118	+
60	62	M	Idiopathic Pulmonary Fibrosis	TAC 4^2, MMF 0.25^2,Pred 10^1	410	-
Summary[c]	**48.4(12.5)**	**M 43.4 %**			**160.1 (73.7)**	**+ 43.4 %**

[a] Days post-transplant

[b] Viral load at time of sampling

[c] Values represent mean or percent of indicated group (SD)

AZA, azathioprine (dose in milligrams); COPD, chronic obstructive pulmonary disease; CSA, cyclosporine (dose in milligrams); F, female; M, male; MMF, mycophenolate mofetil (dose in grams); Pred, prednisone (dose in milligrams); TAC, tacrolimus (dose in milligrams with superscript times per day).